Journal of Applied Physics | PERSPECTIVE | pubs.aip.org/aip/jap

Perspective on defect control in semiconductors for photovoltaics

Cite as: J. Appl. Phys. **134**, 220901 (2023); doi: 10.1063/5.0178959
Submitted: 28 September 2023 · Accepted: 12 November 2023 ·
Published Online: 11 December 2023

Xuefen Cai[1,2] and Su-Huai Wei[2,a)]

AFFILIATIONS

[1]State Key Laboratory of Superlattices and Microstructures, Institute of Semiconductors, Chinese Academy of Sciences, Beijing 100083, China
[2]Beijing Computational Science Research Center, Beijing 100193, China

Note: This paper is part of the Special Topic on Native Defects, Impurities and the Electronic Structure of Compound Semiconductors: A Tribute to Dr. Wladyslaw Walukiewicz.

[a)]**Author to whom correspondence should be addressed:** suhuaiwei@csrc.ac.cn

ABSTRACT

Harnessing the boundless solar energy, photovoltaic cells emerge as pivotal players in the world's sustainable energy landscape. The efficiency of solar cells is intimately tied to the carrier properties influenced by defects and impurities within the sunlight-absorbing semiconductors. In this Perspective, we offer a brief overview of recent advances in exploring doping properties with a focus on three vital thin-film photovoltaic semiconductors: CdTe, CIGS, and halide perovskites. Our discourse encompasses their electronic band structure, intrinsic and extrinsic doping behaviors, defect-assisted nonradiative recombination losses, as well as promising strategies poised to enhance solar cell efficiency. Additionally, we discuss several lingering challenges associated with defects in the advancement of photovoltaic technologies.

I. INTRODUCTION

The ever-growing energy demand propels the pursuit of efficient and sustainable energy solutions. Leveraging the inexhaustible power of solar energy, photovoltaic technology plays an indispensable role in the global energy area. Solar cells, also known as photovoltaic (PV) cells, are devices designed to convert sunlight into electricity through a process called the photovoltaic effect. A sunlight-absorbing semiconductor is the heart of PV cells. Commonly used semiconductors encompass silicon (Si), gallium arsenide (GaAs), cadmium telluride (CdTe), copper indium gallium diselenide [Cu(In, Ga)Se_2, CIGS], halide perovskites, and other related materials, as depicted in Fig. 1(a).[1] Among these, Si-based solar cells dominate the market of installed solar cells.[2,3] However, the crystalline Si solar cells come with relatively high production costs and exhibit low absorption efficiency due to their indirect bandgap. Thus, the search for high-efficiency and cost-effective alternatives to Si is inexorably prompted. GaAs, featuring a direct bandgap of 1.42 eV, boasts an exceptional spectral response characteristic. GaAs-based solar cells have almost supplanted Si in space-level PV modules due to their low weight, high power conversion efficiency (PCE), and impressive performance under radiation conditions.[4] In tandem, CdTe, CIGS, and halide perovskites, endowed with distinct properties and benefits, also receive attention as potent candidates in photovoltaic applications.

The key photovoltaic parameters, namely, the open circuit voltage (V_{oc}), short-circuit current density (J_{sc}), and fill factor (FF), are intricately linked to the carrier density and carrier lifetime of the absorbing materials.[5–7] Specifically, V_{oc}, representing the cell's maximum voltage output, is profoundly connected to the quasi-Fermi-level splitting between electrons and holes, which, in turn, depends on the generated carrier density and their recombination behaviors. J_{sc}, the maximum current generated under short-circuit conditions, is directly impacted by the carrier density—the more the carriers generated, the higher the J_{sc} value. FF, reflecting the cell's effectiveness in utilizing available sunlight, hinges on both carrier density and how long carriers can persist without recombining. Therefore, it is of paramount importance to comprehend and optimize the carrier properties associated with defects and impurities in order to advance photovoltaic efficiencies.

In the context of defects and impurities, as illustrated in Fig. 1(b), the key factors to be examined include the defect

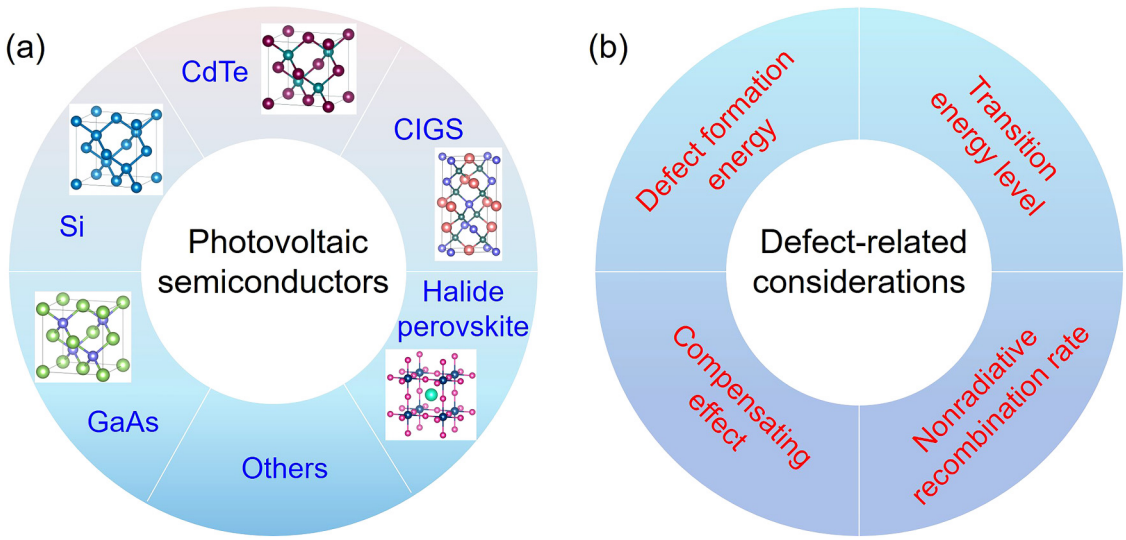

FIG. 1. (a) Common semiconductors used in photovoltaics, featuring Si, GaAs, CdTe, CIGS, and halide perovskites. Corresponding atomic structures are displayed. (b) Fundamental considerations relating to defects for evaluating the quality of photovoltaic materials.

formation energy, transition energy level, self-compensating effect, and defect-induced nonradiative recombination.[8–11] (i) The defect formation energy is a function of Fermi energy and the atomic chemical potentials. This Fermi energy dependence gives rise to the doping limit rule,[9,12,13] which states that materials with a high conduction band minimum (CBM) are difficult to be doped n-type, whereas materials with a low valence band minimum (VBM) are difficult to be doped p-type. (ii) The self-compensating effect can be understood through the concept of amphoteric behavior of native defects, as noted by Dr. Wladek Walukiewicz.[8,14,15] This notion emphasizes that the donor and acceptor native defects compensate one another, resulting in the pinning of the Fermi level at a specific energy level within the semiconductor. (iii) The transition energy level $\varepsilon(q/q')$ represents the Fermi energy at which the formation energy of a defect at charge state q equals that at charge state q'. This parameter characterizes the ionization behavior of dopants at operating temperatures. (iv) In general, defects with deep transition energy levels, located far from the band edges, have the potential to act as nonradiative recombination centers, also known as Shockley–Read–Hall (SRH) recombination centers,[16–20] which can reduce the efficiency of optoelectronic devices like solar cells by diminishing carrier lifetimes.

For decades, extensive research efforts, both experimental and theoretical, have been dedicated to understanding and fine-tuning the properties of defects and impurities in sunlight-absorbing semiconductors, with the goal of enhancing the efficiency of solar cells. These endeavors have yielded significant and notable results. In this Perspective, we aim to illustrate and discuss the substantial advancements in the exploration of defect properties pertaining to three thin-film photovoltaic semiconductors: CdTe, CIGS, and halide perovskites, in conjunction with our recent theoretical research. Specifically, we attempt to outline (i) the intrinsic and group-V doping behaviors in CdTe, along with promising strategies to effectively increase the V_{OC} and J_{SC} values in CdTe solar cells; (ii) the root causes of efficiency drop observed in CIGS solar cells once Ga content exceeds 0.3, highlighting the increasing recombination losses with higher Ga content; and (iii) the atomic structures, inverted band structures, "defect tolerance" notion, and the phenomenon of nonradiative recombination in halide perovskites. This Perspective provides insights into the ongoing efforts to advance the performance of thin-film photovoltaic technologies by addressing key issues related to defects and impurities in these materials.

II. CdTe

CdTe has undergone extensive research since the 1950s and has demonstrated commercial viability as an absorber in thin-film photovoltaics. It boasts various compelling attributes, including cost-effectiveness, efficient high-throughput manufacturing, an appropriate direct bandgap of ~1.5 eV (aligning with maximum efficiency[21]), and a remarkable optical absorption capacity.[22,23] CdTe-based solar cells have reached a notable efficiency record of above 22%,[24] albeit below the 32% Shockley–Queisser limit for single-junction cells.[21,25] This has been mainly attributed to the low hole density (10^{14}–10^{15} cm^{-3}), yielding an open-circuit voltage V_{OC} far below the bandgap at ~0.85 eV, coupled with a short carrier lifetime in the realm of nanoseconds.[5,26,27] These limitations highlight the requirement for refining defect properties within CdTe to enhance its conversion efficiency.

In CdTe, there are six intrinsic point defects involving two vacancies, two interstitials, and two antisites. Our recent Heyd–Scuseria–Ernzerhof (HSE) calculations indicate that Cd vacancy (V_{Cd}) and Te vacancy (V_{Te}) are the dominant intrinsic acceptor

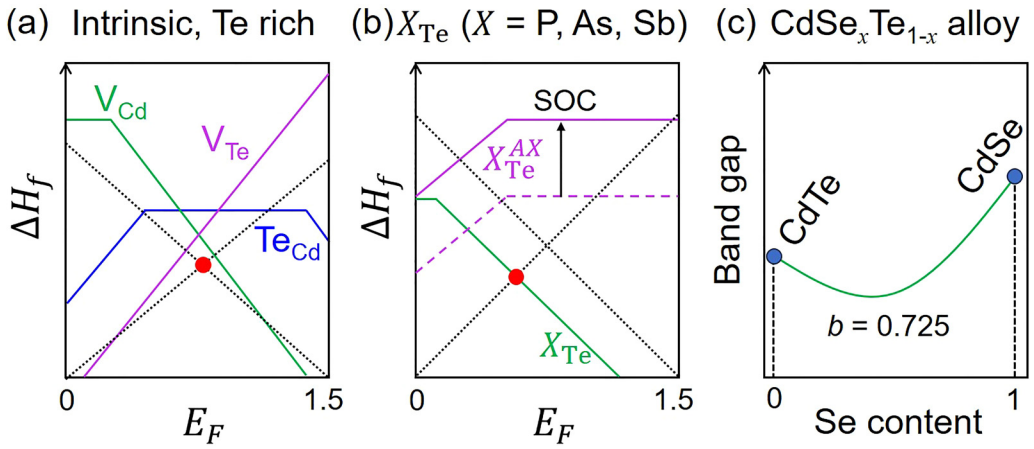

FIG. 2. Schematic diagram of formation energies of (a) intrinsic defects and (b) group-V doping as a function of the Fermi level in CdTe. The band-edge "defects" are shown by black dotted lines. The Fermi-level pinning positions are indicated by red circles. The SOC effect is illustrated by a black arrow. (c) Schematic depiction of bandgap energy of $CdSe_xTe_{1-x}$ alloys as a function of Se content x, with the calculated bowing parameter b noted.

and donor in CdTe, respectively.[28] The formation energies of these two defects as a function of Fermi level under Te-rich conditions are schematically shown in Fig. 2(a). V_{Cd} behaves as a negative-U center with a calculated deep transition energy level $\varepsilon(0/2-)$ located at 0.36 eV above the VBM state. Notably, the neutral charge state of V_{Cd} exhibits a local Jahn–Teller structure distortion, with two neighboring Te atoms drawing closer and the other two moving further apart. On the other hand, V_{Te} is a resonant donor, with its transition energy level $\varepsilon(0/2+)$ positioned above the CBM state.

For p-type doping under Te-rich conditions, V_{Te} acts as a compensating center for V_{Cd}. This compensation process, combined with the thermal excitation of electrons from the band edge (further explanation later), leads to the pinning of the Fermi level at ~0.7 eV [denoted by the red circle in Fig. 2(a)]. While in Te-poor conditions, the formation energies of V_{Cd} and V_{Te} increase and decrease, respectively, ultimately leading to a Fermi level pinning[8] of ~1.3 eV for n-type doping. These pinning Fermi levels remain almost unchanged regardless of the growth temperature. This Fermi level splitting of ~0.6 eV in intrinsic CdTe solar cells grown under equilibrium conditions restricts the V_{oc} value and cell efficiency. To address this limitation, thermodynamic simulations have shown that employing the nonequilibrium quenching method (i.e., growing the sample at high temperature and rapid cooling to room temperature) can significantly lower the Fermi level, enhancing the hole carrier density and potentially enhancing cell performance.[28] Additionally, recent research suggests that nonequilibrium techniques such as illumination could overcome the Fermi-level limitations imposed by the intrinsic compensation effect.[29]

Actually, the V_{oc} value is also constrained by the short minority-carrier lifetime. Through a systematical first-principles study of the nonradiative recombination process in intrinsic p-type CdTe, we suggest that Te on Cd antisite [Te_{Cd}, as schematically depicted in Fig. 2(a)] assumes the dominant recombination center.[30] It exhibits electron capture rate constants B_n and hole capture rate constants B_p of $\sim 10^{-7}$ and $\sim 10^{-6}$ cm^3s^{-1}, respectively, in the context of a two-level recombination process. The calculated results regarding carrier recombination attributed to Te_{Cd} in CdTe fall in line with experimental measurements.[31] On the other hand, recent computational analysis of recombination centers has revealed that V_{Cd} also serves as a trap-assisted recombination center, leading to a decrease in power conversion efficiency by more than 5%.[32] Experimental investigations have characterized the recombination behavior of V_{Cd}.[33,34]

Given the inherent limitations of achieving efficient p-type doping in intrinsic CdTe, it is prudent to explore the use of extrinsic dopants under Te-poor conditions to reduce the formation of the recombination centers. A promising approach has been the incorporation of group-V elements (which have one fewer electron than Te) into the CdTe lattice by replacing Te atoms, thereby forming an acceptor X_{Te} (X = P, As, and Sb). This strategy has shown great potential in enhancing the efficiency of CdTe-based photovoltaic devices, as supported by experiments and first-principles calculations.[35–43] What is not expected is that apart from the role as acceptors, group-V elements may also give rise to AX centers, demoted as X_{Te}^{AX}, which may function as compensating donors for X_{Te} [see Fig. 2(b)].

The calculated results show that X_{Te} is a shallow acceptor with a transition energy level of only ~0.1 eV.[38,44,45] Hybrid functional calculations[46] without accounting for spin–orbit coupling (SOC)[38,45] reveal that the formation energy of X_{Te}^{AX} (delineated by the dashed purple line) is comparable to that of X_{Te}. This suggests that AX centers serve as self-compensation centers for X_{Te}, potentially limiting hole density. Hence, the existence of X_{Te}^{AX} is often utilized to clarify the observed hole density pinning in the range of 10^{16}–10^{17} cm^{-3}, even with the addition of more X into CdTe.[39,40,42] Conversely, when including the effects of spin–orbit coupling in the HSE calculations, pushing up the VBM energy, the AX center is found to be unstable, characterized by a larger formation energy (depicted by the purple line) compared to the desired acceptors

X_{Te}.[47] In this case, X_{Te}^{AX} no longer acts as a dominant compensation center for *p*-type CdTe doped with group-V elements. This raised some hope that group-V doping could further increase hole carrier density. However, detailed balance simulations show that with increased AX formation energies, the Fermi level is still pinned at relatively high energy above the VBM, not much affected by the formation of the AX centers.[48]

To gain a better understanding of defect behaviors in a semiconductor, it is essential to explicitly account for the effects of free carriers in the defect formation energy vs Fermi energy plot for intuitive observations, i.e., treat valence band states as effective donor states and conduction band states as effective acceptor states.[49] The band-edge "defects" induced by free carriers are represented by black dotted lines in Fig. 2(b) [and also Fig. 2(a)]. As one can see, both the effective donor and acceptor states have formation energies close to zero at VBM and CBM, respectively, and their formation energies change linearly with the variation in the Fermi energy. It is noteworthy that due to the charge neutrality requirement, the band-edge "defects" in CdTe serve as the primary sources of compensating "defects," irrespective of the formation of AX centers. Additionally, a recent advancement utilizing the x-ray fluorescence holography technique, as reported by Nagaoka *et al.*, provides a direct insight into the local structure of As dopants in CdTe single crystals.[50] The finding suggests that As substituting on the Cd site (As_{Cd}) may also play a dominant role in self-compensation in As-doped CdTe. Overall, the underlying cause of the hole density pinning issue remains an open question.

Since increasing V_{OC} through optimal defect control is rather difficult in CdTe, another strategy to enhance solar cell performance is by increasing the short-circuit current (J_{SC}). It is well-established that the bandgap of a semiconductor is a critical factor that dictates the energy of photons the material can absorb. In principles, when the bandgap is strategically slightly reduced while remaining within the optimal range of 1.2–1.5 eV,[21] the semiconductor can capture longer wavelengths of sunlight. That is, a smaller bandgap broadens the spectrum of sunlight that the semiconductors can utilize, thereby increasing J_{SC}. Recent research, employing HSE + SOC calculations, has demonstrated that alloying a certain amount of CdSe into CdTe can narrow the bandgap from 1.48 to 1.39 eV, despite CdSe having a larger bandgap than CdTe.[51] This bandgap reduction can potentially increase the J_{SC} in photovoltaic devices, falling in line with recent experimental findings.[52–54] The primary cause of this bandgap narrowing is attributed to the bowing effect,[55] as illustrated schematically in Fig. 2(c). Importantly, a significant portion of this bandgap reduction is observed to originate from the downward shift of the conduction band minimum. As a result, the sacrifice of V_{OC} is expected to be relatively small. Furthermore, this research has revealed that the alloy formation of $CdSe_xTe_{1-x}$ (CdSeTe) will likely reduce the effective formation energy[56] of shallow acceptors like Cu_{Cd} due to strain effects.[57] This reduction can enhance *p*-type doping and consequently improve V_{OC}.

In fact, the CdSeTe alloy has already been integrated into CdTe devices, contributing to the attainment of the latest record efficiency.[24,58,59] While the J_{sc} is essentially maxed out, the enhanced V_{oc} still lags behind its theoretical capacity, potentially hindered by several factors: (i) point defects and defect complexes that serve as compensating defects or recombination centers;[41,60–62] and (ii) band tailing (sub-bandgap absorption), caused by inhomogeneity and electrostatic fluctuations in *p*-type CdSeTe, resulting in a reduction in the open-circuit voltage.[63] A deeper understanding of Se-related defect physics in CdSeTe holds promise for driving further improvements in performance.

III. $Cu(In, Ga)Se_2$

Chalcopyrite-based solar cells, also known as CIGS solar cells, have garnered significant attention in the photovoltaic industry owing to their impressive efficiency, which has reached up to 23.4% to date.[64] Initially, $CuInSe_2$ (CIS) was employed as the absorbing material in chalcopyrite-based solar cells primary due to its high sunlight absorption coefficient of $\sim 10^5\ cm^{-1}$.[65,66] However, CIS's bandgap of just 1.04 eV falls short of the optimal range for achieving maximum efficiency in single-junction PVs.[21] To address this limitation, $CuGaSe_2$ (CGS), boasting a bandgap of 1.68 eV, is often alloyed with CIS to form $Cu(In,Ga)Se_2$ (CIGS), allowing for the fine-tuning of the bandgap and enhancing the overall performance of these solar cells, as schematically plotted in Fig. 3(a). Regarding the advancements in CIGS solar cells, it is noteworthy that the PCE initially increases with the introduction of Ga into CIS as expected but decreases when the Ga/(Ga + In) ratio exceeds about 0.3. That is, the peak PCE of CIGS solar cells is achieved at a Ga concentration of around 30% with a bandgap of around 1.2 eV.[67–71] Improving the efficiency of CIGS solar cells necessitates a comprehensive understanding of the factors limiting their performance. Both experimental and theoretical studies have been conducted to uncover the origins of these limitations.[70,72–77]

Intrinsic CIS and CGS are *p*-type doping materials[64,78,79] due to their high-energy antibonding character of VBM states composed of Cu *d* and Se *p* orbitals.[80,81] Previous theoretical findings indicated that the low-formation-energy copper vacancy (V_{Cu}) serves as the effective shallow acceptor in both CIS and CGS,[72,73,80] as depicted schematically in Fig. 3(b). Since the VBM states of both CIS and CGS exhibit similarities and Ga and In *p* orbital energies are similar, the addition of Ga does not alter the defect properties of V_{Cu}. Thus, V_{Cu} remains the dominant acceptor, leading to the *p*-type doping with varying Ga compositions. Conversely, the antisite defect M_{Cu} (M = In and Ga) forms donor levels in both CIS and CGS and becomes deeper when the Ga concentration increases in CIGS, mainly due to the increase in the CBM energy of CGS compared to that of CIS.[80] As Ga_{Cu} and In_{Cu} transition energy levels become progressively deeper in CIGS, it was speculated that M_{Cu} functions as effective recombination centers in CIGS with relatively high Ga composition, potentially accounting for the efficiency decrease when the Ga concentration exceeds 30%.

However, when a defect level moves away from the CBM, the electron capture rate is expected to be reduced, not enhanced. This causes a dilemma whether M_{Cu} is an effective recombination center. Previous theoretical calculations have revealed that merely assessing the position of defect levels within the bandgap is insufficient for evaluating the defect-induced nonradiative recombination abilities.[11,82] Indeed, first-principles calculations of nonradiative recombination coefficients indicate that the antisite M_{Cu} alone cannot induce efficient nonradiative capture coefficients in CIGS; it

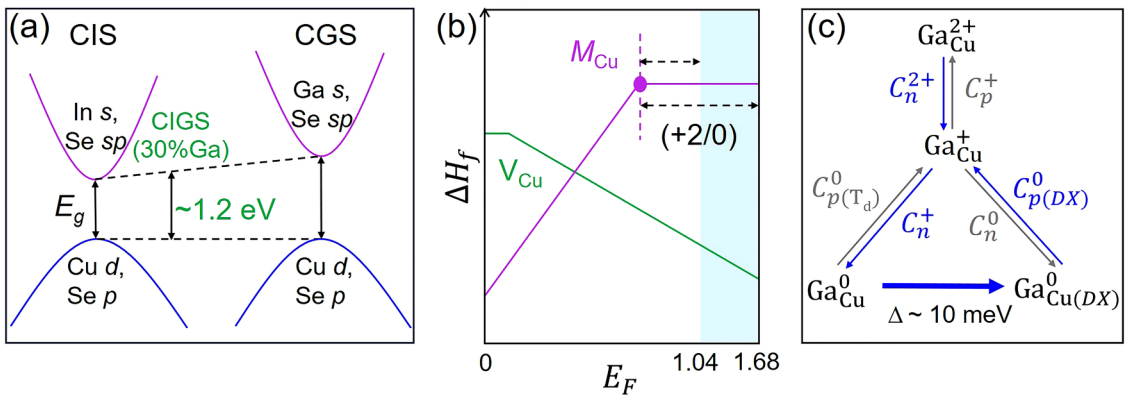

FIG. 3. Schematic illustrations. (a) Electrical band structures in CIGS: The purple and blue parabolas represent the CB and VB states, respectively. The main components of band edges are marked. (b) Formation energies of V_{Cu} and M_{Cu} in CIS and CGS: This plot depicts the formation energies of the dominant acceptor V_{Cu} and antisite donor M_{Cu} (M = In and Ga) as a function of the Fermi level in CIS and CGS. The zero of the Fermi level is at the VBM of both compounds. Black dashed lines schematically indicate the deeper donor level in CGS compared to that in CIS. (c) Nonradiative recombination processes of Ga_{Cu} in CGS: The dominant processes are indicated by blue arrows.

can efficiently capture electrons but not holes.[83] Instead, an efficient hole capture process can only be obtained when M^0_{Cu} forms the DX centers denoted as $M^0_{Cu(DX)}$. In $M^0_{Cu(DX)}$, one M–Se bond is broken, making the local symmetry change from T_d to C_{3v}, and the energy level becomes much closer to the VBM.

Figure 3(c) schematically illustrates the nonradiative recombination process of Ga_{Cu} in CGS.[83] In CGS, the calculated hole capture coefficient at room temperature for the DX center $C^0_{p(DX)}$ is $\sim 10^{-9}$ cm^{3}s^{-1}, significantly higher than that of the common antisite $C^0_{p(T_d)}$ of only $\sim 10^{-24}$ cm^{3}s^{-1}. Given the low energy barrier (Δ) from the neutral antisite to the DX center (only 10 meV), the neutral antisite can transition to the DX center spontaneously. The blue arrows in Fig. 3(c) indicate the main recombination process. The complete $Ga^+_{Cu} \leftrightarrow Ga^0_{Cu}$ recombination transition is attained through the following cycle: $[Ga^+_{Cu} + e^- + h^+] \rightarrow [Ga^0_{Cu} + h^+] \rightarrow [Ga^0_{Cu(DX)} + h^+] \rightarrow [Ga^+_{Cu}]$. In short, the internal conversion from the neutral charge state to the DX center configuration creates an efficient hole capture route, leading to large recombination losses. Note that the DX center is energetically stable in CGS and high-Ga-composition CIGS but not in low-Ga-concentration CIGS and CIS primarily due to the relatively low CBM of CIS compared to CGS. Therefore, the number of recombination losses induced by the antisite M_{Cu} is indeed Ga-content-dependent. These findings provide a deeper understanding of the efficiency drop observed in CIGS solar cells as Ga concentration exceeds 30%[70] and suggest that to reduce the recombination, one may have to grow the sample under the Cu-rich condition to decrease the concentration of M_{Cu} in CIGS.

IV. HALIDE PEROVSKITE

Low-cost halide perovskite solar cells have demonstrated a remarkable increase in power efficiency, surging from 3.8%[84] to well beyond 25%[85,86] since their inception in 2009. Halide perovskites adopt a chemical formula of ABX_3, wherein A represents a monovalent cation. This category includes both organic entities like $CH(NH_2)_2^+$ (formamidinium, FA^+) and $CH_3NH_3^+$ (methylammonium, MA^+) and inorganic ions such as Cs^+. Components B and X typically denote a metal cation like Pb^{2+} or Sn^{2+} and a negatively charged halide anion (Cl^-, Br^-, and I^-), respectively.[87–90] Halide perovskites crystallize in many different polymorphs such as the α (cubic), β (tetragonal), and γ (orthorhombic) phases. Figure 4(a) depicts the cubic α phase with a space group of $Pm\bar{3}m$.[91] The cation B atom is centered on the BX_6 octahedra surrounded by six halide atoms. The octahedra interconnects by mutually sharing the corner X atoms. The cation A is located in the space between the corner-sharing PbO_6 octahedra. The other phases exhibit different extents of tilting and distortions of the perfect BX_6 octahedra. The perovskite lattice is softer than many conventional semiconductors.[92,93] If a photoactive perovskite phase transitions to nonphotoactive phases, the photovoltaic performance naturally vanishes.[94,95] Thus, enhancing the stability of photoactive perovskite is vital. The thermodynamic stability of perovskite structures has frequently been predicted through the Goldschmidt tolerance factor (t),[96] namely,

$$t = \frac{r_A + r_X}{\sqrt{2}(r_B + r_X)}, \tag{1}$$

where r_A, r_B, and r_X are the ionic radii of A, B, and X species, respectively. Empirically, a tolerance factor ranging from 0.8 to 1.0 indicates a photoactive perovskite phase.[97]

Halide perovskites typically have a direct bandgap with both VBM and CBM situated at the R point.[91,98–100] Unlike the conventional semiconductors like GaAs and CdTe, which feature a p-like VBM and an s-like CBM, the VBM states of perovskites are constructed from the antibonding state between the B lone-pair ns^2 and halogen p orbitals, while the CBM states are dominated by the B p nonbonding states.[101–104] Notably, cation A has minimal

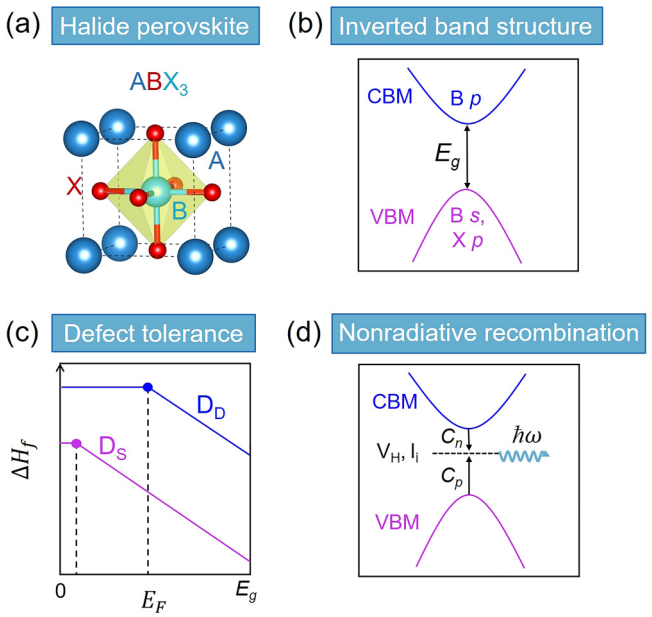

FIG. 4. Schematic representation of (a) the atomic structure of halide perovskites ABX_3, along with (b) unique band structure, (c) "defect tolerance" concept, and (d) the presence of nonradiative recombination centers such as V_H and I_i. The VBM and CBM states are depicted as purple and blue parabolas, respectively. The hole capture coefficient C_p and electron capture coefficient C_n are also indicated.

influence on the band edge states. Given that *p* states possess two more orbitals and manifest less dispersion in comparison to *s* states, the direct *p*–*p* optical transition in perovskites inherently tends to yield a larger joint density of states (JDOS) and stronger optical absorption than other solar cell absorbers with *p*–*s* optical transition. To illustrate, the calculated optical absorption coefficient of $CH_3NH_3PbI_3$ surpasses that of GaAs by approximately one order of magnitude.[91]

In the last few decades, substantial research has been dedicated to the defect properties of halide perovskites. Early research demonstrates a gratifying characteristic of "defect tolerance" in halide perovskites.[93,103,105,106] Specifically, shallow defects (D_S) tend to have a relatively modest formation energy, while deep defects (D_D) exhibit significantly higher formation energies within the perovskite structure, as illustrated in Fig. 4(c). Additionally, both experimental and theoretical investigations have found that perovskite materials such as $CsPbI_3$ and $CH_3NH_3PbI_3$ can effectively attain both *p*- and *n*-type doping by manipulating the chemical potential.[104,107–109] Undoubtedly, these intriguing defect properties are intimately intertwined with the structural and electronic properties.[93,103,110,111] As stated above, the VBM of halide perovskite predominantly emerges from the antibonding combination of the B *s* and X *p* orbitals. This gives rise to a high-energy VBM, thereby leading to the formation of dominant shallow acceptors (such as V_{Pb} and MA_{Pb} in $MAPbI_3$). On the other hand, the shallow donors (such as MA_i and V_I in $MAPbI_3$) are potentially attributed to the large atomic size of the constituent atoms and the ionic nature of the MA–X bond. Moreover, the strong SOC interaction, facilitated by heavy atoms like Pb, lowers the CBM energy level and reduces the energy gain of the DX-like center, promoting the formation of shallow donors. The high efficiency of halide perovskite solar cells has been commonly attributed to their exceptional defect tolerance properties and high optical absorption.

However, recent first-principles calculations asserted the presence of energetically favorable deep point defects that serve as nonradiative recombination centers within halide perovskites,[82,112–114] as schematically represented in Fig. 4(d). This raises some questions about the defect tolerance aforementioned. This disparity has been ascribed to the divergence in computational approaches. Recent studies have harnessed hybrid functionals[46] along with SOC, whereas early ones employed semilocal exchange-correlation functionals without considering the SOC effect.[115] Thorough examinations of defects within $MAPbI_3$ have indicated that iodine interstitials (I_i) and hydrogen vacancies (V_H) are the predominant nonradiative recombination centers.[82,113] Since I_i and V_H become plentiful under I-rich and I-poor conditions, respectively, an I-medium condition is conducive to improving the performance of hybrid perovskite solar cells. Regarding $FAPbI_3$, it has been observed that the formation energy of V_H is comparably high. As such, the non-radiative recombination originating from V_H in $FAPbI_3$ is notably weaker than that in $MAPbI_3$, underscoring the crucial role of FA in attaining high performance in hybrid perovskites.[116–118] However, it is worth noting that $FAPbI_3$ exhibits lower phase stability compared to $MAPbI_3$.[87,116,119] Given these insights, alloying $MAPbI_3$ and $FAPbI_3$ emerges as a promising approach, potentially yielding a delicate balance between nonradiative recombination and phase stability, thus fostering an enhancement in overall device performance.

V. CONCLUSION AND OUTLOOK

To conclude, we have provided an overview of the significant strides in the recent study of defect properties within three pivotal thin-film photovoltaic semiconductors: CdTe, CIGS, and halide perovskites. In the domain of CdTe, research on intrinsic defects has revealed that the efficiency of cells based on intrinsic CdTe is primarily limited by factors including the deep level of the dominant acceptor V_{Cd}, the self-compensating nature of donor V_{Te}, and the recombination losses induced by Te_{Cd}. The utilization of group-V doping and the formation of $CdSe_xTe_{1-x}$ alloys emerge as promising approaches for enhancing the V_{OC}, $J_{SC,}$ and, ultimately, the conversion efficiency. However, the Fermi energy pinning caused by intrinsic defects and "band edge" defects should be carefully studied. As for CIGS, its intrinsic *p*-type doping behavior can be attributed to the high VBM states composed of antibonding Cu *d* orbitals. The introduction of Ga into $CuInSe_2$ to form CIGS alloy initially boosts efficiency by widening the bandgap. However, excessive Ga into CIS significantly reduces efficiency due to the formation of $M^0_{Cu(DX)}$ centers, which increases recombination losses induced by M_{Cu} as the Ga content increases. New growth conditions (e.g., Cu-rich) and architecture may be required to overcome this issue. Concerning organic–inorganic halide perovskites, the well-known "defect tolerance" notion is caused by its high ionicity

and *s–p* antibonding character near the VBM. However, the organic molecules involved in these compounds make the defect control more complicated because each element in the molecules can be a potential source of defects and recombination centers, as shown in the recent observations of nonradiative recombination behaviors.

While the insights gained regarding defect properties in these critical PV semiconductors hold promise for enhancing solar cell performance, it is crucial to acknowledge that some persisting unresolved issues and challenges demand further investigation in future research: (i) the primary source of compensation in group-V-doped CdTe thin films observed in experiments remain an open question.[39,40,42,120] Various compensation mechanisms, including the well-known AX center, defect complex, secondary phase, impurity clusters, and alternative possibilities, warrant thorough examination. (ii) Halide perovskites have relatively low defect densities compared to most conventional thin-film solar cell materials. However, recent studies of carrier recombination suggest that halide perovskites may not be inherently defect-tolerant.[82,112–114] Determining the main cause behind this distinctive feature remains an ongoing inquiry. (iii) To date, first-principles investigations into defect properties in solar cells have mainly focused on those within the absorber layer. Yet, defect-related phenomena in other layers, such as the transparent conducting oxide layer[121] and at the surface and interfaces of different layers, need further exploration. (iv) Considering that carrier compensation is an intrinsic problem that is always difficult to overcome under thermodynamic equilibrium conditions,[8,9,122] better understanding of the non-equilibrium doping processes, such as light illumination,[29,123–126] the applications of external electric and magnetic fields, within these PV materials need to be systematically assessed.

Certainly, a comprehensive understanding of defect properties in PV semiconductors plays a pivotal role in enhancing the efficiency of PV devices. Of note, this understanding calls for advances in high-level computational methods, sophisticated experimental technologies, and well-established concepts and models.

ACKNOWLEDGMENTS

This work was supported by the National Natural Science Foundation of China (NNSFC) (Grants Nos. 12204471, 11991060, 12088101, and U2230402). The authors dedicate this work to the memory of Dr. Wladek Walukiewicz, who made important contributions to understanding defect physics in semiconductors and was a good friend of one of the authors (S.-H.W.).

AUTHOR DECLARATIONS

Conflict of Interest

The authors have no conflicts to disclose.

Author Contributions

Xuefen Cai: Data curation (equal); Formal analysis (equal); Funding acquisition (equal); Investigation (equal); Validation (equal); Visualization (equal); Writing – original draft (equal); Writing – review & editing (equal). **Su-Huai Wei:** Conceptualization (equal); Data curation (equal); Formal analysis (equal); Funding acquisition (equal); Investigation (equal); Project administration (equal); Resources (equal); Supervision (equal); Validation (equal); Visualization (equal); Writing – original draft (equal); Writing – review & editing (equal).

DATA AVAILABILITY

The data that support the findings of this study are available from the corresponding author upon reasonable request.

REFERENCES

[1]V. Mohanapriya and V. Manimegalai, in *Electrical and Electronic Devices, Circuits, and Materials* (John Wiley & Sons, Ltd., 2021), pp. 299–314.
[2]T. Saga, NPG Asia Mater. **2**, 96 (2010).
[3]R. Schmalensee, Energy Econ. **52**, S142 (2015).
[4]M. Bosi and C. Pelosi, Prog. Photovolt. Res. Appl. **15**, 51 (2007).
[5]J. Sites and J. Pan, Thin Solid Films **515**, 6099 (2007).
[6]A. Kanevce and T. A. Gessert, IEEE J. Photovolt. **1**, 99 (2011).
[7]H.-X. Deng, R. Cao, and S.-H. Wei, Sci. China Phys. Mech. **64**, 237301 (2021).
[8]W. Walukiewicz, Appl. Phys. Lett. **54**, 2094 (1989).
[9]S.-H. Wei, Comput. Mater. Sci. **30**, 337 (2004).
[10]C. Freysoldt, B. Grabowski, T. Hickel, J. r. Neugebauer, G. Kresse, A. Janotti, and C. G. Van de Walle, Rev. Mod. Phys. **86**, 253 (2014).
[11]X. Zhang, J. X. Shen, and C. G. Van de Walle, Adv. Energy Mater. **10**, 1902830 (2020).
[12]S. B. Zhang, S.-H. Wei, and A. Zunger, J. Appl. Phys. **83**, 3192 (1998).
[13]S. B. Zhang, S. H. Wei, and A. Zunger, Phys. Rev. Lett. **84**, 1232 (2000).
[14]W. Walukiewicz, J. Vac. Sci. Technol. B **5**, 1062 (1987).
[15]W. Walukiewicz, Phys. Rev. B **37**, 4760 (1988).
[16]R. N. Hall, Phys. Rev. **87**, 387 (1952).
[17]W. Shockley and W. T. Read, Phys. Rev. **87**, 835 (1952).
[18]C.-T. Sah, R. N. Noyce, and W. Shockley, Proc. IRE **45**, 1228 (1957).
[19]C. H. Henry and D. V. Lang, Phys. Rev. B **15**, 989 (1977).
[20]A. M. Stoneham, Rep. Prog. Phys. **44**, 1251 (1981).
[21]W. Shockley, and H. J. Queisser, J. Appl. Phys. **32**, 510 (1961).
[22]J. J. Loferski, J. Appl. Phys. **27**, 777 (1956).
[23]M. Afzaal and P. O'Brien, J. Mater. Chem. **16**, 1597 (2006).
[24]See https://www.nrel.gov/pv/cell-efficiency.html for "Best Research-Cell Efficiency Chart" (accessed September 2023).
[25]C. H. Henry, J. Appl. Phys. **51**, 4494 (1980).
[26]T. A. A. Gessert, S. H. Wei, J. Ma, D. S. Albin, R. G. Dhere, J. N. Duenow, D. Kuciauskas, A. Kanevce, T. M. Barnes, J. M. Burst, W. L. Rance, M. O. Reese, and H. R. Moutinho, Sol. Energy Mater. Sol. Cells **119**, 149 (2013).
[27]M. A. Green, E. D. Dunlop, M. Yoshita, N. Kopidakis, K. Bothe, G. Siefer, and X. Hao, Prog. Photovolt. Res. Appl. **31**, 651 (2023).
[28]J.-H. Yang, J.-S. Park, J. Kang, W. Metzger, T. Barnes, and S.-H. Wei, Phys. Rev. B **90**, 245202 (2014).
[29]X. Cai, J.-W. Luo, S.-S. Li, S.-H. Wei, and H.-X. Deng, Phys. Rev. B **106**, 214102 (2022).
[30]J.-H. Yang, L. Shi, L.-W. Wang, and S.-H. Wei, Sci. Rep. **6**, 21712 (2016).
[31]D. Kuciauskas, A. Kanevce, P. Dippo, S. Seyedmohammadi, and R. Malik, IEEE J. Photovolt. **5**, 366 (2015).
[32]S. R. Kavanagh, A. Walsh, and D. O. Scanlon, ACS Energy Lett. **6**, 1392 (2021).
[33]D. Kuciauskas, P. Dippo, Z. Zhao, L. Cheng, A. Kanevce, W. K. Metzger, and M. Gloeckler, IEEE J. Photovolt. **6**, 313 (2016).
[34]D. Kuciauskas and D. Krasikov, IEEE J. Photovolt. **8**, 1754 (2018).
[35]M. Zandian, A. C. Chen, D. D. Edwall, J. G. Pasko, and J. M. Arias, Appl. Phys. Lett. **71**, 2815 (1997).

[36]C. Kraft, A. Brömel, S. Schönherr, M. Hädrich, H. Metzner, U. Reislöhner, P. Schley, G. Gobsch, R. Goldhahn, and W. Wesch, Thin Solid Films **519**, 7153 (2011).
[37]J. M. Burst, J. N. Duenow, D. S. Albin, E. Colegrove, M. O. Reese, J. A. Aguiar, C. S. Jiang, M. K. Patel, M. M. Al-Jassim, D. Kuciauskas, S. Swain, T. Ablekim, K. G. Lynn, and W. K. Metzger, Nat. Energy **1**, 16015 (2016).
[38]J.-H. Yang, W.-J. Yin, J.-S. Park, J. Ma, and S.-H. Wei, Semicond. Sci. Technol. **31**, 083002 (2016).
[39]E. Colegrove, J. H. Yang, S. P. Harvey, M. R. Young, J. M. Burst, J. N. Duenow, D. S. Albin, S. H. Wei, and W. K. Metzger, J. Phys. D: Appl. Phys. **51**, 075102 (2018).
[40]B. E. McCandless, W. A. Buchanan, C. P. Thompson, G. Sriramagiri, R. J. Lovelett, J. Duenow, D. Albin, S. Jensen, E. Colegrove, J. Moseley, H. Moutinho, S. Harvey, M. Al-Jassim, and W. K. Metzger, Sci. Rep. **8**, 14519 (2018).
[41]A. Nagaoka, D. Kuciauskas, J. McCoy, and M. A. Scarpulla, Appl. Phys. Lett. **112**, 192101 (2018).
[42]G. Kartopu, O. Oklobia, D. Turkay, D. R. Diercks, B. P. Gorman, V. Barrioz, S. Campbell, J. D. Major, M. K. Al Turkestani, S. U. Yerci, T. M. Barnes, N. S. Beattie, G. Zoppi, S. Jones, and S. J. C. Irvine, Sol. Energy Mater. Sol. Cells **194**, 259 (2019).
[43]W. K. Metzger, S. Grover, D. Lu, E. Colegrove, J. Moseley, C. L. Perkins, X. Li, R. Mallick, W. Zhang, R. Malik, J. Kephart, C.-S. Jiang, D. Kuciauskas, D. S. Albin, M. M. Al-Jassim, G. Xiong, M. Gloeckler, Nat. Energy **4**, 837 (2019).
[44]S.-H. Wei and S. B. Zhang, Phys. Rev. B **66**, 155211 (2002).
[45]B. Dou, Q. Sun, and S.-H. Wei, Phys. Rev. Appl. **15**, 054045 (2021).
[46]J. Heyd, G. E. Scuseria, and M. Ernzerhof, J. Chem. Phys. **118**, 8207 (2003).
[47]I. Chatratin, B. Dou, S.-H. Wei, and A. Janotti, J. Phys. Chem. Lett. **14**, 273 (2023).
[48]J. H. Park, S. Farrell, R. Kodama, C. Blissett, X. Wang, E. Colegrove, W. K. Metzger, T. A. Gessert and S. Sivananthan, J. Electron. Mater. **43**, 2998 (2014).
[49]J.-H. Yang, W.-J. Yin, J.-S. Park, and S.-H. Wei, Sci. Rep. **5**, 16977 (2015).
[50]A. Nagaoka, K. Kimura, A. K. R. Ang, Y. Takabayashi, K. Yoshino, Q. Sun, B. Dou, S.-H. Wei, K. Hayashi, and K. Nishioka, J. Am. Chem. Soc. **145**, 9191 (2023).
[51]J. Yang and S.-H. Wei, Chin. Phys. B **28**, 086106 (2019).
[52]N. R. Paudel and Y. Yan, Appl. Phys. Lett. **105**, 183510 (2014).
[53]N. R. Paudel, J. D. Poplawsky, K. L. Moore, and Y. Yan, IEEE J. Photovolt. **5**, 1492 (2015).
[54]J. D. Poplawsky, W. Guo, N. Paudel, A. Ng, K. More, D. Leonard, and Y. Yan, Nat. Commun. **7**, 12537 (2016).
[55]S.-H. Wei, S. B. Zhang, and A. Zunger, J. Appl. Phys. **87**, 1304 (2000).
[56]J. Ma and S.-H. Wei, Phys. Rev. B **87**, 241201 (2013).
[57]J. Zhu, F. Liu, G. B. Stringfellow, and S.-H. Wei, Phys. Rev. Lett. **105**, 195503 (2010).
[58]M. A. Scarpulla, B. McCandless, A. B. Phillips, Y. Yan, M. J. Heben, C. Wolden, G. Xiong, W. K. Metzger, D. Mao, D. Krasikov, I. Sankin, S. Grover, A. Munshi, W. Sampath, J. R. Sites, A. Bothwell, D. Albin, M. O. Reese, A. Romeo, M. Nardone, R. Klie, J. M. Walls, T. Fiducia, A. Abbas, and S. M. Hayes, Sol. Energy Mater Sol. Cells **255**, 112289 (2023)..
[59]D. Krasikov, Nat. Energy **4**, 442 (2019).
[60]D. Krasikov and I. Sankin, J. Mater. Chem. A **5**, 3503 (2017).
[61]D. Krasikov and I. Sankin, Phys. Rev. Mater. **2**, 103803 (2018).
[62]A. Nagaoka, D. Kuciauskas, and M. A. Scarpulla, Appl. Phys. Lett. **111**, 232103 (2017).
[63]J. Moseley, S. Grover, D. Lu, G. Xiong, H. L. Guthrey, M. M. Al-Jassim, and W. K. Metzger, J. Appl. Phys. **128**, 103105 (2020).
[64]M. Nakamura, K. Yamaguchi, Y. Kimoto, Y. Yasaki, T. Kato, and H. Sugimoto, IEEE J. Photovolt. **9**, 1863 (2019).
[65]G. X. Liang, P. Fan, Z. H. Zheng, J. T. Luo, D. P. Zhang, J. R. Chi, C. M. Chen, and J. Zhao, Adv. Mat. Res. **734**, 2480 (2013).
[66]B. Rehani, J. R. Ray, C. J. Panchal, H. Master, R. R. Desai, and P. B. Patel, J. Nano-Electron. Phys. **5**, 02007(4pp) (2013).
[67]H.-W. Schock and R. Noufi, Prog. Photovolt. Res. Appl. **8**, 151 (2000).
[68]M. A. Contreras, K. Ramanathan, J. AbuShama, F. Hasoon, D. L. Young, B. Egaas, and R. Noufi, Prog. Photovolt. Res. Appl. **13**, 209 (2005).
[69]T. Eisenbarth, T. Unold, R. Caballero, C. A. Kaufmann, D. Abou-Ras, and H. W. Schock, Thin Solid Films **517**, 2244 (2009).
[70]M. A. Contreras, L. M. Mansfield, B. Egaas, J. Li, M. Romero, R. Noufi, E. Rudiger-Voigt, and W. Mannstadt, in *37th IEEE Photovoltaic Specialists Conference* (IEEE, Seattle, WA, 2011), p. 000026.
[71]S. Merdes, R. Mainz, J. Klaer, A. Meeder, H. Rodriguez-Alvarez, H. W. Schock, M. C. Lux-Steiner, and R. Klenk, Sol. Energy Mater. Sol. Cells **95**, 864 (2011).
[72]S.-H. Wei, S. B. Zhang, and A. Zunger, Appl. Phys. Lett. **72**, 3199 (1998).
[73]S. B. Zhang, S.-H. Wei, A. Zunger, and H. Katayama-Yoshida, Phys. Rev. B **57**, 9642 (1998).
[74]S. Lany and A. Zunger, Phys. Rev. Lett. **93**, 156404 (2004).
[75]S.-H. Wei and S. B. Zhang, J. Phys. Chem. Solids **66**, 1994 (2005).
[76]S. Lany and A. Zunger, Phys. Rev. Lett. **100**, 016401 (2008).
[77]A. Chirilă, S. Buecheler, F. Pianezzi, P. Bloesch, C. Gretener, A. R. Uhl, C. Fella, L. Kranz, J. Perrenoud, S. Seyrling, R. Verma, S. Nishiwaki, Y. E. Romanyuk, G. Bilger, and A. N. Tiwari, Nat. Mater. **10**, 857 (2011).
[78]R. N. Bhattacharya, W. Batchelor, J. F. Hiltner, and J. R. Sites, Appl. Phys. Lett. **75**, 1431 (1999).
[79]P. K. Johnson, J. T. Heath, J. D. Cohen, K. Ramanathan, and J. R. Sites, Prog. Photovolt. Res. Appl. **13**, 579 (2005).
[80]B. Huang, S. Chen, H.-X. Deng, L.-W. Wang, M. A. Contreras, R. Noufi, and S.-H. Wei, IEEE J. Photovolt. **4**, 477 (2014).
[81]H. Yu, X. Cai, Y. Yang, Z.-H. Wang, and S.-H. Wei, Comput. Mater. Sci. **203**, 111157 (2022).
[82]X. Zhang, M. E. Turiansky, J.-X. Shen, and C. G. Van de Walle, Phys. Rev. B **101**, 140101 (2020).
[83]B. Dou, S. Falletta, J. R. Neugebauer, C. Freysoldt, X. Zhang, and S.-H. Wei, Phys. Rev. Appl. **19**, 054054 (2023).
[84]A. Kojima, K. Teshima, Y. Shirai, and T. Miyasaka, J. Am. Chem. Soc. **131**, 6050 (2009).
[85]J. Jeong, M. Kim, J. Seo, H. Lu, P. Ahlawat, A. Mishra, Y. Yang, M. A. Hope, F. T. Eickemeyer, M. Kim, Y. J. Yoon, I. W. Choi, B. P. Darwich, S. J. Choi, Y. Jo, J. H. Lee, B. Walker, S. M. Zakeeruddin, L. Emsley, U. Rothlisberger, A. Hagfeldt, D. S. Kim, M. Grätzel, and J. Y. Kim, Nature **592**, 381 (2021).
[86]Y. Zhao, F. Ma, Z. Qu, S. Yu, T. Shen, H.-X. Deng, X. Chu, X. Peng, Y. Yuan, X. Zhang, and J. You, Science **377**, 531 (2022).
[87]N. J. Jeon, J. H. Noh, W. S. Yang, Y. C. Kim, S. Ryu, J. Seo, and S. I. Seok, Nature **517**, 476 (2015).
[88]D. Bi, W. Tress, M. I. Dar, P. Gao, J. Luo, C. m. Renevier, K. Schenk, A. Abate, F. Giordano, J.-P. Correa Baena, J.-D. Decoppet, S. M. Zakeeruddin, M. K. Nazeeruddin, M. Grätzel, and A. Hagfeldt, Sci. Adv. **2**, e1501170 (2016).
[89]J.-P. Correa-Baena, M. Saliba, T. Buonassisi, M. Grätzel, A. Abate, W. Tress, and A. Hagfeldt, Science **358**, 739 (2017).
[90]W. S. Yang, B.-W. Park, E. H. Jung, N. J. Jeon, Y. C. Kim, D. U. Lee, S. S. Shin, J. Seo, E. K. Kim, J. H. Noh, and S. I Seok, Science **356**, 1376 (2017).
[91]W.-J. Yin, T. Shi, and Y. Yan, Adv. Mater. **26**, 4653 (2014).
[92]F. Brivio, J. M. Frost, J. M. Skelton, A. J. Jackson, O. J. Weber, M. T. Weller, A. R. Goñi, A. l. M. A. Leguy, P. R. F. Barnes, and A. Walsh, Phys. Rev. B **92**, 144308 (2015).
[93]J. Kang and L.-W. Wang, J. Phys. Chem. Lett. **8**, 489 (2017).
[94]C. C. Stoumpos, C. D. Malliakas, and M. G. Kanatzidis, Inorg. Chem. **52**, 9019 (2013).
[95]R. Jinnouchi, J. Lahnsteiner, F. Karsai, G. Kresse, and M. Bokdam, Phys. Rev. Lett. **122**, 225701 (2019).
[96]V. M. Goldschmidt, Naturwissenschaften **14**, 477 (1926).
[97]M. Saliba, T. Matsui, K. Domanski, J.-Y. Seo, A. Ummadisingu, S. M. Zakeeruddin, J.-P. Correa-Baena, W. R. Tress, A. Abate, A. Hagfeldt, and M. Grätzel, Science **354**, 206 (2016).

[98]F. Brivio, K. T. Butler, A. Walsh, and M. Van Schilfgaarde, Phys. Rev. B **89**, 155204 (2014).
[99]E. Menéndez-Proupin, P. Palacios, P. Wahnón, and J. C. Conesa, Phys. Rev. B **90**, 045207 (2014).
[100]H. M. Ghaithan, Z. A. Alahmed, S. M. H. Qaid, M. Hezam, and A. S. Aldwayyan, ACS Omega **5**, 7468 (2020).
[101]S.-H. Wei and A. Zunger, Phys. Rev. B **55**, 13605 (1997).
[102]A. Walsh, D. J. Payne, R. G. Egdell, and G. W. Watson, Chem. Soc. Rev. **40**, 4455 (2011).
[103]W.-J. Yin, T. Shi, and Y. Yan, Appl. Phys. Lett. **104**, 063903 (2014).
[104]W.-J. Yin, J.-H. Yang, J. Kang, Y. Yan, and S.-H. Wei, J. Mater. Chem. A **3**, 8926 (2015).
[105]A. Buin, P. Pietsch, J. Xu, O. Voznyy, A. H. Ip, R. Comin, and E. H. Sargent, Nano Lett. **14**, 6281 (2014).
[106]K. X. Steirer, P. Schulz, G. Teeter, V. Stevanovic, M. Yang, K. Zhu, and J. J. Berry, ACS Energy Lett. **1**, 360 (2016).
[107]L. Etgar, P. Gao, Z. Xue, Q. Peng, A. K. Chandiran, B. Liu, M. K. Nazeeruddin, and M. Grätzel, J. Am. Chem. Soc. **134**, 17396 (2012).
[108]W. A. Laban and L. Etgar, Energy Environ. Sci. **6**, 3249 (2013).
[109]J. You, Z. Hong, Y. Yang, Q. Chen, M. Cai, T.-B. Song, C.-C. Chen, S. Lu, Y. Liu, and H. Zhou, ACS Nano **8**, 1674 (2014).
[110]R. E. Brandt, J. R. Poindexter, P. Gorai, R. C. Kurchin, R. L. Z. Hoye, L. Nienhaus, M. W. B. Wilson, J. A. Polizzotti, R. Sereika, R. Žaltauskas, L. C. Lee, J. L. MacManus-Driscoll, M. Bawendi, V. Stevanović, and T. Buonassisi, Chem. Mater. **29**, 4667 (2017).
[111]J. Kang, J. Li, and S.-H. Wei, Appl. Phys. Rev. **8**, 031302 (2021).
[112]M. W. Swift and J. L. Lyons, J. Mater. Chem. A **9**, 7491 (2021).
[113]X. Zhang, J.-X. Shen, M. E. Turiansky, and C. G. Van de Walle, Nat. Mater. **20**, 971 (2021).
[114]X. Zhang and S.-H. Wei, Phys. Rev. Lett. **128**, 136401 (2022).
[115]X. Zhang, M. E. Turiansky, J.-X. Shen, and C. G. Van de Walle, J. Appl. Phys. **131**, 090901 (2022).
[116]H. Min, M. Kim, S.-U. Lee, H. Kim, G. Kim, K. Choi, J. H. Lee, and S. I. Seok, Science **366**, 749 (2019).
[117]G. Kim, H. Min, K. S. Lee, D. Y. Lee, S. M. Yoon, and S. I. Seok, Science **370**, 108 (2020).
[118]H. Lu, Y. Liu, P. Ahlawat, A. Mishra, W. R. Tress, F. T. Eickemeyer, Y. Yang, F. Fu, Z. Wang, C. E. Avalos, B. I. Carlsen, A. Agarwalla, X. Zhang, X. Li, Y. Zhan, S. M. Zakeeruddin, L. Emsley, U. Rothlisberger, L. Zheng, A. Hagfeldt, and M. Grätzel, Science **370**, eabb8985 (2020).
[119]M. Saliba, T. Matsui, J.-Y. Seo, K. Domanski, J.-P. Correa-Baena, M. K. Nazeeruddin, S. M. Zakeeruddin, W. Tress, A. Abate, A. Hagfeldt, and M. Grätzel, Energy Environ. Sci. **9**, 1989 (2016).
[120]A. Nagaoka, K. Nishioka, K. Yoshino, R. Katsube, Y. Nose, T. Masuda, and M. A. Scarpulla, Appl. Phys. Lett. **116**, 132102 (2020).
[121]X. Cai and S.-H. Wei, Appl. Phys. Lett. **119**, 070502 (2021).
[122]S. B. Zhang, S.-H. Wei, and A. Zunger, Physica B **273–274**, 976 (1999).
[123]K. Alberi and M. A. Scarpulla, Sci. Rep. **6**, 27954 (2016).
[124]P. Reddy, M. P. Hoffmann, F. Kaess, Z. Bryan, I. Bryan, M. Bobea, A. Klump, J. Tweedie, R. Kirste, S. Mita, M. Gerhold, R. Collazo, and Z. Sitar, J. Appl. Phys. **120**, 185704 (2016).
[125]K. Alberi and M. A. Scarpulla, J. Appl. Phys. **123**, 185702 (2018).
[126]A. Klump, M. P. Hoffmann, F. Kaess, J. Tweedie, P. Reddy, R. Kirste, Z. Sitar, and R. Collazo, J. Appl. Phys. **127**, 045702 (2020).